Preparing Low-Surface-Energy Polymer Materials by Minimizing Intermolecular Hydrogen-Bonding Interactions

Shiao-Wei Kuo,*,† Yi-Chen Wu,† Chih-Feng Wang,‡ and Kwang-Un Jeong§

Department of Materials and Optoelectronic Science, Center for Nanoscience and Nanotechnology, National Sun Yat-Sen University, Kaohsiung, 804, Taiwan, Department of Materials Science and Engineering, I-Shou University, 84041 Kaohsiung, Taiwan, and Department of Polymer-Nano Science and Technology, Chonbuk National University, Jeonju 561-756, Korea

Received: June 25, 2009; Revised Manuscript Received: October 15, 2009

In this study, we found that poly(vinyl phenol)/polybenzoxazine (PVPh/PBZ) copolymers feature low surface energies when they possess a minimal number of intermolecular hydrogen-bonding interactions. For example, PVPh/PBZ = 30/70 exhibits an extremely low surface energy of 16.8 mJ/m^2 after thermal curing—even lower than that of poly(tetrafluoroethylene) (22.0 mJ/m^2)—based on calculations performed using a two-liquid geometric method. Infrared spectroscopic analyses indicated that a decrease in the degree of intermolecular hydrogen bonding in the PVPh/PBZ copolymers resulted in a lower surface free energy. An increase in the intermolecular hydrogen bonding did, however, enhance the thermal properties, namely, the glass-transition temperature, the thermal decomposition temperature, and the char yield. The manipulation of intermolecular hydrogen-bonding interactions is a unique and simple approach toward preparing low-surface-energy materials without the need to employ fluoropolymers or silicones.

Introduction

The performance of polymeric materials is often dictated by their surface properties, such as wettability, friction, and adhesion. A low surface energy is important for many practical applications of polymers. Much of the commercial success of poly(dimethylsiloxane) (PDMS) and poly(tetrafluoroethylene) (PTFE) arises from their low surface energies.[1−4] PTFE may be regarded as the benchmark low-surface-energy material; it combines water repellency[5] with other desirable properties.[6] The small size, high electronegativity, and low polarizability of fluorine atoms and strong fluorine−fluorine repulsion[7] result in weak intermolecular forces between fluorinated polymer chains and, thus, relatively low surface energies. Nevertheless, PTFE and many other fluorinated polymers have limited applicability because of their high costs and poor processability. Much effort has been exerted in the search for low-cost polymeric materials exhibiting low surface free energies, ready processability, and good film-forming characteristics.[8−10]

Amorphous comblike polymers possessing flexible linear backbones on the side chains with weak intermolecular interactions generally exhibit low surface energies.[11] Chung et al.[12] reported that the presence of amide groups in fluorinated main-chain liquid-crystalline polymer systems tends to induce strong intermolecular hydrogen bonding, resulting in higher surface energies and hydrophilicity. Wang et al. reported that polybenzoxazines (PBZs) are a new class of nonfluorine, nonsilicon, low-surface-free-energy polymeric materials because of their intramolecular hydrogen bonding of six-membered rings;[8] they have a wide range of applications as superhydrophobic surfaces,[13−15] in lithographic patterning,[16] and as mold-release materials in nanoimprint technology.[17] Notably, intermolecular hydrogen bonding between the hydroxyl (OH) groups in PBZ systems increases their surface energies.[8] Lin et al. discovered that poly(vinyl phenol) (PVPh) also possesses an extremely low surface energy (15.7 mJ/m^2), even lower than that of PTFE (22.0 mJ/m^2), after simple thermal treatment because of a decrease in the degree of intermolecular hydrogen bonding between its OH groups.[18] The nature of the pendant chains has a most profound effect in determining the surface energy of a material; indeed, low-surface-free-energy materials can be obtained by decreasing the intermolecular interactions of comblike polymers possessing flexible linear backbones.[19]

Hydrogen bonds can be formed both intermolecularly and intramolecularly. An intramolecular hydrogen bond forms when the hydrogen bond donor and acceptor are parts of the same molecule; an intermolecular hydrogen bond is formed between two different molecules. In polymer chains, the same functional group can form either interchain or intrachain hydrogen bonds.[20,21] For example, the α-helix and β-sheet structures of polypeptides are stabilized through intrachain and interchain hydrogen bonds, respectively.[22,23] The relationship between the surface free energy and the degrees of intermolecular or intramolecular hydrogen bonding remains poorly understood. Because PVPh and PBZ possess low surface free energies,[8,18] we were interested in whether their blends would also have similar properties. Interestingly, Wang et al. found that the surface energies of PBZ systems cured at 180 °C generally decrease upon increasing the curing time due to the formation of strong intramolecular hydrogen bonds.[8] Similarly, Lin et al. found that PVPh possesses extremely low surface energy after thermal treatment at 180 °C.[18] In general terms, thermal treatment at high temperatures tends to disrupt hydrogen bonds such that they reform in different distributions (inter- and intramolecular hydrogen bonded, free) after rapid cooling to ambient temperature. However, the intramolecular hydrogen-bonded structure of polybenzoxazine is very stable even as high of a temperature as 300 °C, whereas the intermolecular hydrogen

* To whom correspondence should be addressed. E-mail: kuosw@faculty.nsysu.edu.tw. Phone: 886-7-5252000, ext. 4079. Fax: 886-7-5254099.
† National Sun Yat-Sen University.
‡ I-Shou University.
§ Chonbuk National University.

10.1021/jp9059642 CCC: $40.75
Published on Web 11/10/2009

SCHEME 1: Possible Reactions between Benzoxazine and PVPh

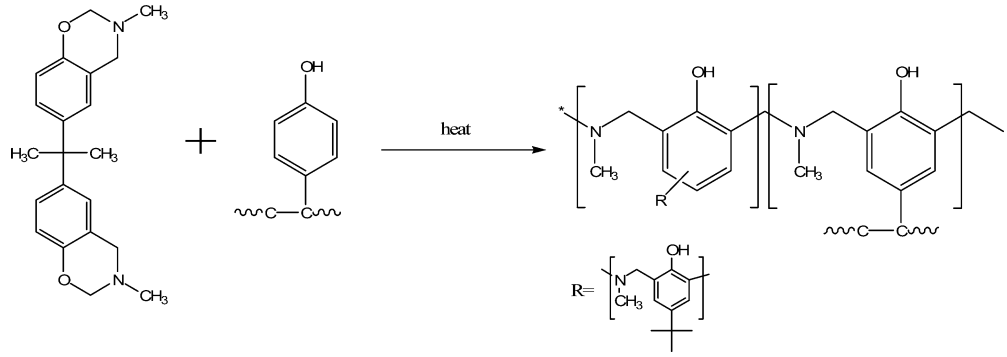

bonding weakens even at the glass transition (*T*g) temperature.[24−29] As a result, we suspected that blends of PBZ and PVPh in various compositions would change their original surface energies when treated at 180 °C for various lengths of time to mediate the intermolecular hydrogen bonding. We note that PBZ will react with PVPh through its phenolic OH groups such that the blend system will behave as a simple thermoset composite (Scheme 1).

Previous studies[8,11,12,18] have suggested that an increase in the degree of intramolecular hydrogen bonding will decrease the surface energy of a polymeric material. In contrast, the increase in the degree of intermolecular hydrogen bonding generally enhances the thermal properties, such as the glass-transition temperature (T_g), decomposition temperature (T_d), and char yield, of a polymer blend or copolymer system, as we have discussed in several previous reports.[30−37] Therefore, we suspected that measurements of the surface free energies and thermal properties of polymer blends and copolymer systems might help us to distinguish the relationship between the surface free energies and the degree of hydrogen bonding. To the best of our knowledge, this paper is the first report of a material exhibiting a low surface energy as a result of controlling its hydrogen-bonding interactions by physical polymer blending. Furthermore, we have used differential scanning calorimetry (DSC), thermogravimetric analysis (TGA), dynamic mechanical analysis (DMA), and Fourier transform infrared (FTIR) spectroscopy to characterize the chemical structure, thermal properties, and specific interactions within these PVPh/PBZ copolymer systems.

Experimental Section

Materials. The PVPh used in this study was prepared through living anionic polymerization of 4-*tert*-butoxystyrene and subsequent removal of the *tert*-butoxy protective group through selective hydrolysis.[25,26,30] 2,2-bis(3,4-dihydro-3-methyl-2*H*-1,3-benzoxazine)propane (BA-m benzoxazine) was supplied by Shikoku Chemicals Corp. (Japan). PVPh/benzoxazine blends of various compositions were prepared through THF solution blending. The solution was filtered through a 0.2 μm syringe filter before spin-coating onto a glass by immediate spinning at 1500 rpm for 45 s.; they were then cured at 180 °C for 4 h under vacuum to ensure total curing of the benzoxazine.

Characterization. The glass-transition temperatures (T_g) of the polymer blend were determined through DSC using a TA Q-20 instrument. To observe the curing behavior, the scan rate was 20 °C/min within the temperature range from 30 to 300 °C. FTIR spectra of the polymer blend films were recorded using the conventional KBr disk method. A THF solution containing the blend was cast onto a KBr disk, and the films used in this study were sufficiently thin to obey the Beer−Lambert law. FTIR spectra were recorded using a Bruker Tensor 27 FTIR spectrophotometer; 32 scans were collected at a spectral resolution of 1 cm^{-1}. FTIR spectra recorded at elevated temperatures were obtained using a cell mounted inside the temperature-controlled compartment of the spectrometer. Generalized two-dimensional (2D) correlation analysis was performed using the 2D Shige software developed by Shigeaki Morita (Kwansei-Gakuin University, Japan). In 2D correlation maps, red-colored regions are defined as having positive correlation intensities and blue-colored regions are defined as having negative correlation intensities. A TA Instruments Q50 thermogravimetric analyzer (scan rate = 20 °C, from 30 to 800 °C, nitrogen purge = 40 mL/min) was used to record TGA thermograms of the samples positioned on a platinum holder. DMA was performed using a PerkinElmer Instruments DMA 8000 apparatus operated in tension mode over a temperature range from 30 to 400 °C. Analyses of the loss tangent (tan δ) were recorded automatically by the system. The heating rate and frequency were fixed at 2 °C/min and 1 Hz, respectively. Surface roughness profiles of the film structures were acquired using a Digital Instruments DI5000 scanning probe microscope operated in the tapping mode. Values of root mean square (rms) roughness were calculated over scan areas of 5 μm × 5 μm. A Krüss GH-100 goniometer interfaced to image-capture software was used to measure the advancing contact angles of the samples at 25 °C; a liquid drop of deionized water or diiodomethane (5 μL) was injected onto the polymer surface. A two-liquid geometric method was employed to determine the surface energy.[38]

Results and Discussion

Surface Free Energy Analyses. Table 1 lists the surface roughnesses, advancing contact angles, and surface free energies of all of the tested specimens after thermally activated polymerization at 180 °C for 4 h. Because the surface roughness of each specimen was less than 20 nm, the influence of the topography on the surface free energy was negligible. The advancing contact angle is generally less sensitive to surface roughness and heterogeneity than the receding angle; therefore, advancing contact angle data are commonly used to calculate the components of the surface and interfacial tension.[39,40] After simple thermal treatment, the fluorine- and silicone-free pure PVPh (18.6 mJ/m^2) and pure PBZ(Ba-m) (18.04 mJ/m^2) systems exhibited significantly lower surface free energies than that of PTFE (22.0 mJ/m^2) when using the same testing liquids and calculation method.[41]

Figure 1 summarizes the surface free energies of the PVPh/PBZ copolymer blends after thermally activated polymerization

TABLE 1: Surface Free Energy, Hydrogen-Bonding Interactions, and Thermal Properties of PVPh/PBZ Copolymer Systems

		contact angle				thermal property			thermal curing	
polymers	roughness (nm)	H_2O	DIM	γ (mJ/m^2)	f_{HB}^{OH-O} (%)	T_g (°C)	T_d (°C)	char (wt %)	T_p	ΔH_{curing} (J/g)
PBZ	7.8	105.5	79.8	18.6	16.0	187	380	36.8	213.3	346.9
PVPh/PBZ=20/80	8.2	109.3	82.0	17.1	43.4	182	373	31.8	207.5	317.7
PVPh/PBZ=30/70	4.3	111.1	81.9	16.8	41.0	185	381	34.7	209.1	361.4
PVPh/PBZ=40/60	7.1	99.4	71.9	22.5	41.6	166	394	40.7	209.8	409.5
PVPh/PBZ=50/50	5.6	103.9	60.6	28.8	41.9	242	398	46.0	191.6	475.4
PVPh/PBZ=60/40	6.3	86.4	54.8	34.6	49.1	347	410	47.8	190.9	435.2
PVPh/PBZ=70/30	4.7	95.5	55.6	31.9	49.8	304	395	44.1	187.5	390.3
PVPh/PBZ=80/20	8.4	95.8	60.0	29.8	49.6	294	378	36.9	186.6	337.5
PVPh	5.9	107.7	78.6	18.1	44.0	217	366	20.2	186.1	

at 180 °C for 4 h. The surface free energy first decreased upon increasing the PVPh content within the range from 20 to 30 wt %. Indeed, PVPh/PBZ = 30/70 exhibited the lowest surface energy (16.8 mJ/m^2) among all of the blends—even lower than those of their pure parent polymers. The surface free energy increased upon further increasing the PVPh content from 40 to 60 wt %—indeed, the highest surface energy occurred at PVPh/PBZ = 60/40 (34.6 mJ/m^2)—and then it decreased again upon increasing the PVPh content from 70 to 100 wt %. To understand the mechanisms behind the surface free energy changes of these PVPh/PBZ copolymers, we characterized them in terms of their FTIR spectra.

FTIR Spectroscopic Analyses. As a first step, we sought to determine the thermally activated polymerization mechanism of the PVPh/BA-m = 50/50 mixture at 180 °C for various curing times (Figure 2). The significant decreases in intensity of the bands at 1232 and 948 cm^{-1}, which indicate the presence of the benzoxazine ring,[42] implied that the ring-opening reactions had occurred. This result was confirmed by the appearance of a new distribution of bands within the range of 3600−3100 cm^{-1}, which we assign to the hydrogen-bonded OH units of the opened oxazine ring species. In addition, a new band for the tetrasubstituted aromatic ring of the polymerized BA-m appears at 1480 cm^{-1}, with a corresponding decrease in the intensity of the band, representing the trisubstituted aromatic ring of BA-m (1498 cm^{-1}). Figure 3 displays expanded FTIR spectra (3800−2800 cm^{-1}) for pure PVPh, pure PBZ, and various PVPh/PBZ copolymers after thermal curing at 180 °C for 4 h. For pure PVPh, the OH band can be fitted by four Gaussian functions (Figure 3h): a narrower shoulder band at 3650−3580 cm^{-1}, representing the free OH group; a peak at 3550−3515 cm^{-1}, representing the OH−π weak hydrogen bonding; a peak at 3450−3350 cm^{-1}, representing hydrogen-bonded OH group in linear chains; and a peak at 3230−3110 cm^{-1} is corresponding to the OH groups involved in hydrogen-bonded "dimers" (OH···OH) and a signal for OH groups involved in multiple hydrogen-bonding interactions for cyclic structures.[43] For pure PBZ, three different kinds of hydrogen bonds were evident (Figure 3a): OH···O intermolecular hydrogen bonds (ca. 3420 cm^{-1}), OH···N intramolecular hydrogen bonds (ca. 3200 cm^{-1}), and O$^-$···H$^+$N intramolecular hydrogen bonds (ca. 2750 cm^{-1}), which have all been discussed in a previous report.[44] Figure 3 presents the corresponding curve fitting results for the various PVPh/PBZ copolymers. Here, we assign five different kinds of OH groups present in the PVPh/PBZ copolymers: free OH groups (ca. 3630 cm^{-1}), intramolecular OH···π hydrogen-bonded (ca. 3550 cm^{-1}), intermolecular OH···O hydrogen-bonded (ca. 3420 cm^{-1}), multiple intramolecular OH···OH hydrogen-bonded (3300 cm^{-1}), and intramolecular OH···N hydrogen-bonded (ca. 3200 cm^{-1}). Increasing the degree of intermolecular hydrogen bonding of a polymeric material tends to increase its surface energy.[8,12] Figure 1 and Table 1 compare the area fractions of intermolecular hydrogen bonded species in the PVPh/PBZ copolymers with their surface free energies. A general trend is that an increase

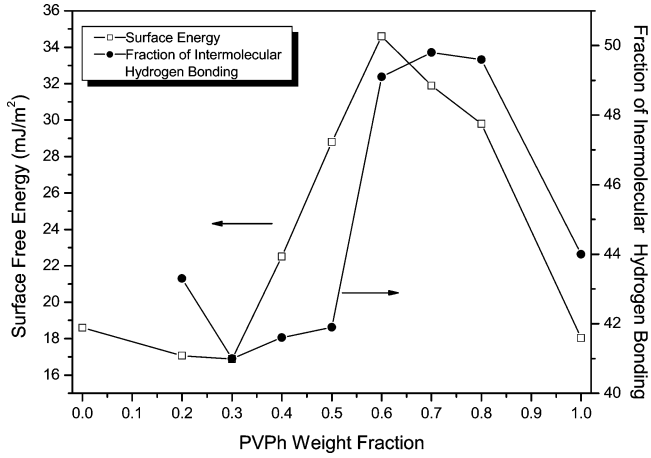

Figure 1. Surface free energy and fraction of intermolecular hydrogen bonds in PVPh/PBZ copolymers containing various PVPh contents.

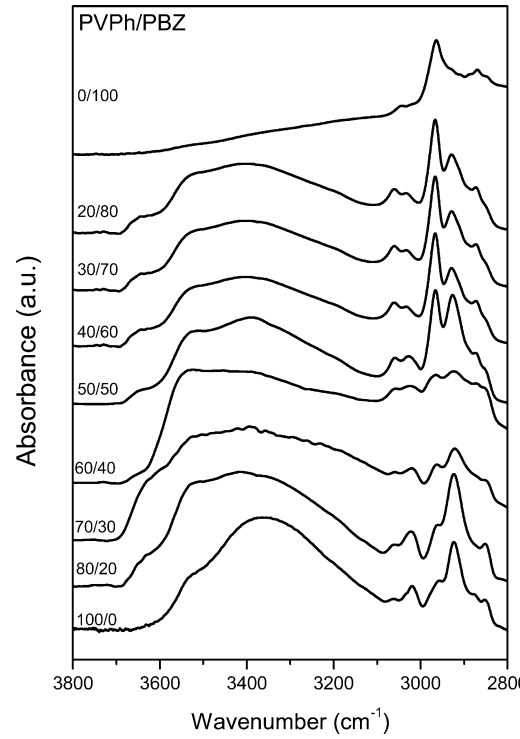

Figure 2. FTIR spectra of PVPh/PBZ copolymers containing various PVPh contents, recorded at room temperature.

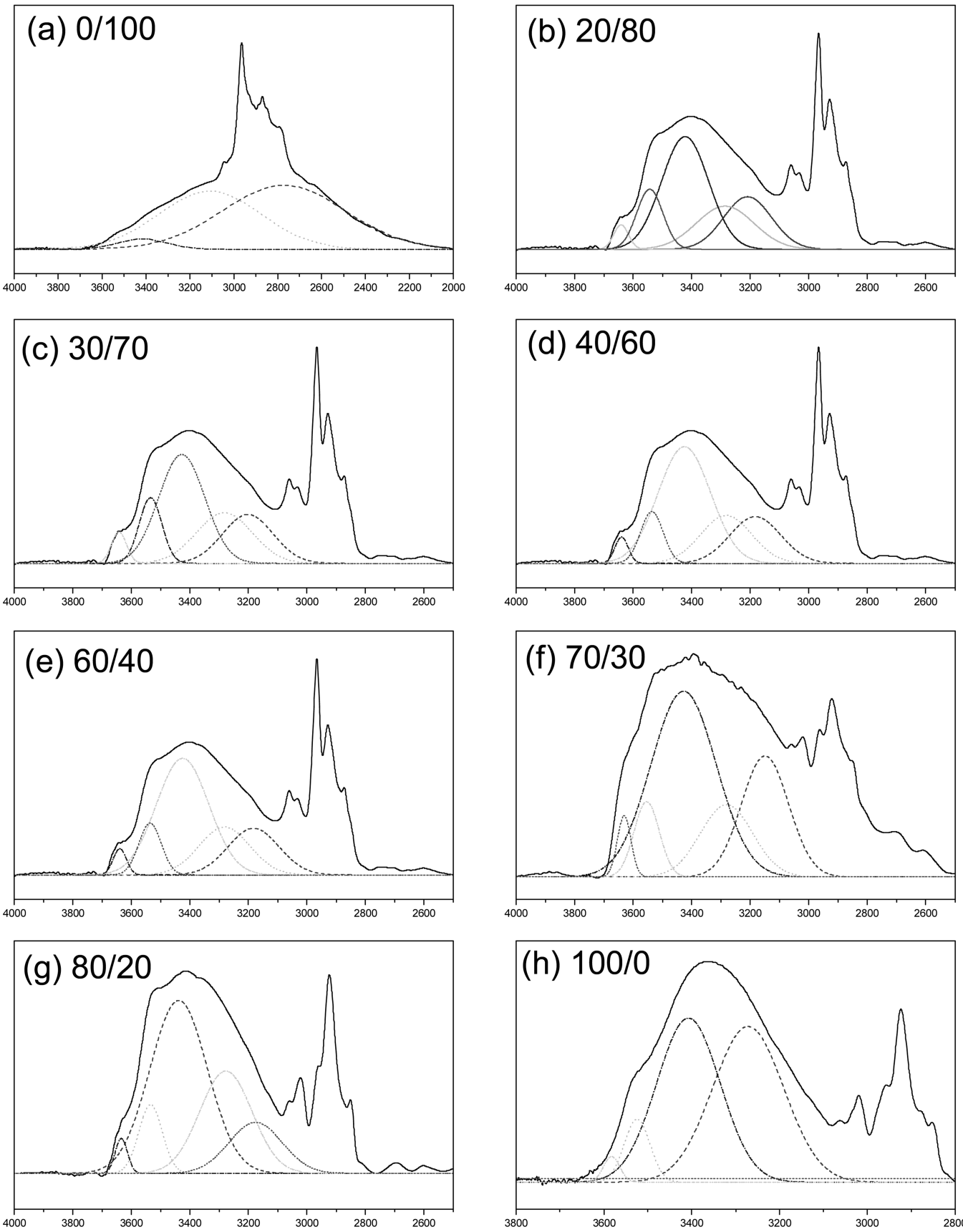

Figure 3. Curve fitting of the room-temperature FTIR spectroscopic data of PVPh/PBZ copolymers containing various PVPh contents.

in the degree of intermolecular hydrogen bonding led to a higher surface free energy for the PVPh/PBZ copolymers.

Wang et al. reported that the curing time influences the surface free energy of PBZ; they found that the lowest surface free

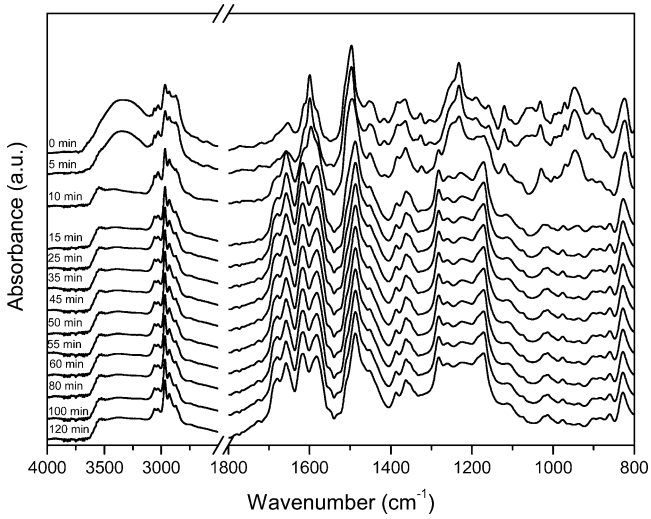

Figure 4. FTIR spectra of PVPh/PBZ = 80/20 copolymers after treatment at 180 °C for various curing times.

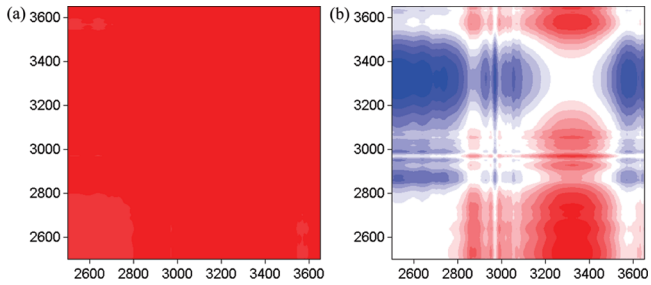

Figure 5. (a) Synchronous and (B) asynchronous 2D maps of the FTIR spectroscopic data for PVPh/PBZ copolymers treated for various curing times.

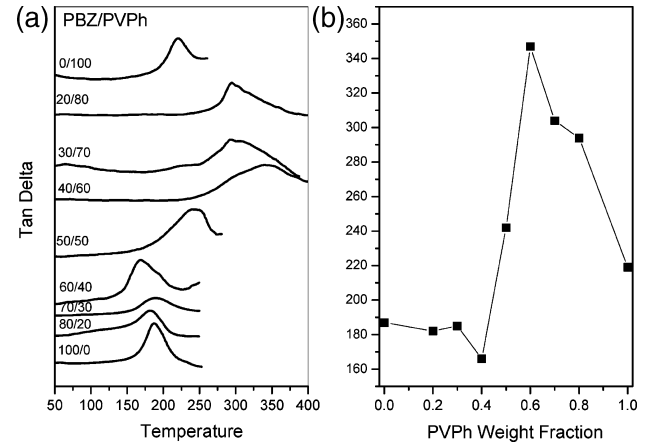

Figure 6. (a) DMA analyses and (b) resulting glass-transition behavior of PBZ/PVPh copolymers containing various PVPh contents.

energy occurred after curing at 210 °C for 1 h because of the minimal extent of OH···O intermolecular hydrogen bonding.[8] The area fraction of these hydrogen bonds increased upon increasing the curing time. It is clear that enhanced intramolecular hydrogen bonding leads to a decrease in the surface free energy and an increase in the water contact angle. Figure 4 shows FTIR spectra of PVPh/PBZ = 80/20 copolymers after treatment at 180 °C for various curing times. Clearly, a new band for the tetrasubstituted aromatic ring of the polymerized BA-m appears at 1480 cm^{-1} with a corresponding decrease in the intensity of the band representing the trisubstituted aromatic ring of BA-m (1498 and 943 cm^{-1}) assigned to the trisubstituted benzene ring in the benzoxazine structure were found to

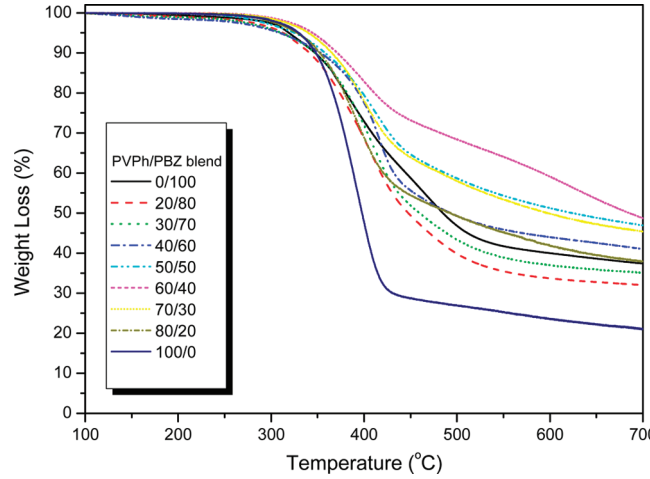

Figure 7. TGA analyses of PVPh/PBZ copolymers containing various PVPh contents.

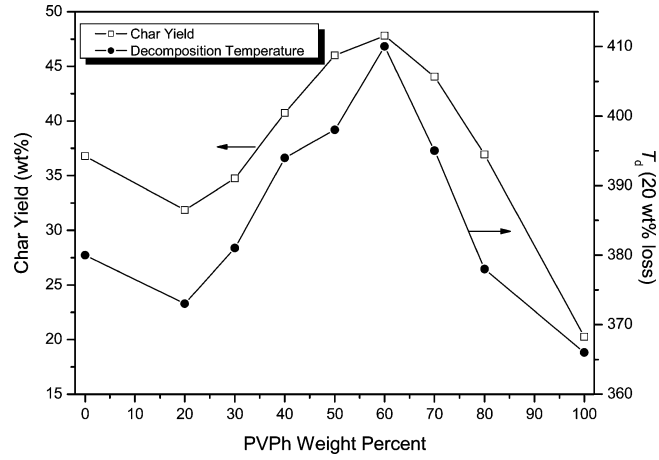

Figure 8. Values of T_d and char yields of PVPh/PBZ copolymers containing various PVPh contents.

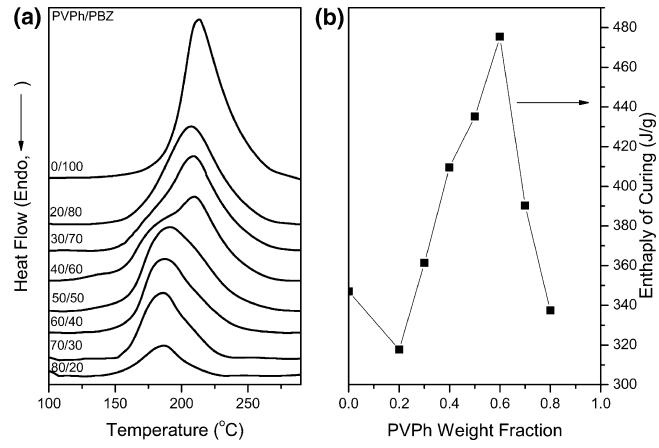

Figure 9. (a) Curing behavior determined through DSC analyses and (b) enthalpies of curing of PVPh/PBZ copolymers containing various PVPh contents.

disappear at a much early state of the cure (ca. 10−15 min). We used 2D correlation spectroscopy to further characterize the changes in the nature of the interactions of this copolymer system after the various curing times. This approach has been applied widely in polymer science[45−48] to investigate the specific interactions between polymer chains by treating the spectral fluctuations as a function of time, temperature, pressure, and composition. Red and blue areas in 2D IR correlation contour

maps represent positive and negative cross-peaks, respectively. In general, two types of spectra, 2D synchronous and asynchronous, are obtained; the correlation intensities in the 2D synchronous and asynchronous maps reflect the relative degrees of in-phase and out-of-phase responses, respectively. The 2D synchronous spectra are symmetric with respect to the diagonal line in the correlation map. Autopeaks, which represent the degree of autocorrelation of perturbation-induced molecular vibrations, are located at the diagonal positions of a synchronous 2D spectrum; their values are always positive. When an autopeak appears, the signal at that wavenumber would change greatly under environmental perturbation. Cross-peaks located at off-diagonal positions of a synchronous 2D spectrum (they may be positive or negative) represent the simultaneous or coincidental changes of the spectral intensity variations measured at ν_1 and ν_2. Positive cross-peaks result when the intensity variations of the two peaks at ν_1 and ν_2 occur in the same direction (i.e., both increase or both decrease) under the environmental perturbation; negative cross-peaks reveal that the intensities of the two peaks at ν_1 and ν_2 change in opposite directions (i.e., one increases while the other decreases) under perturbation.[45]

As in the case for a synchronous spectrum, the sign of an asynchronous cross-peak can be either negative or positive, providing useful information on the sequential order of events observed by the spectroscopic technique along the external variable. The 2D asynchronous spectra are asymmetric with respect to the diagonal line in the correlation map. According to Noda's rule,[45] when $\Phi(\nu_1,\nu_2) > 0$, if $\psi(\nu_1,\nu_2)$ is positive (black-colored area), band ν_1 will vary prior to band ν_2; if $\psi(\nu_1,\nu_2)$ is negative (white-colored area), band ν_2 will vary prior to band ν_1. This rule is reversed, however, when $\Phi(\nu_1,\nu_2) < 0$. In summary, if the symbols of the cross-peak in the synchronous and asynchronous maps are the same (both positive or both negative), band ν_1 will vary prior to band ν_2; if the symbols of the cross-peak are different in the synchronous and asynchronous spectra (one positive and the other negative), band ν_1 will vary after ν_2 under the environmental perturbation.

Figure 5a presents the synchronous 2D correlation maps in the range of 3700−2500 cm^{-1}. The absorption bands present in this spectral range have been assigned above. Clear, positive cross-peaks existed between all of the signals from 3700 to 2500 cm^{-1}, implying that they all proceed in the same direction (increase together) upon increasing the curing time, according to Noda's rule, because of the degree of thermal curing increased upon increasing the curing time.[38] Figure 5b displays the asynchronous 2D correlation maps in the range of 3700−2500 cm^{-1}. We observe no auto- or cross-peaks within the ranges of 3400−3200 cm^{-1} (OH···N) and 2700−2500 cm^{-1} (O^-···H^+N), implying that intramolecular hydrogen bonding existed in these spectral ranges, consistent with our previous assignments. The cross-peaks between the signals at 3400−3200 cm^{-1} and those at 3600−3420 cm^{-1} in Figure 5b exhibit opposing intensity orders, indicating that these two bands result from different polymer chains, that is, intramolecular OH···N hydrogen-bonding, intermolecular OH···O hydrogen-bonding, and free OH groups. In addition, the positive peaks at 3400−3200 cm^{-1} in the asynchronous 2D map in Figure 5b imply that the intensity of the peak at 3200 cm^{-1} (OH···N) altered before that at 3420 cm^{-1} (OH···O) upon increasing the curing time. This finding—that the formation of intramolecular OH···N hydrogen bonds occurs first, resulting in a lower surface free energy, and then they change to intermolecular OH···O hydrogen bonds upon increasing the curing time, thereby tending to increase the surface free energy—is consistent with the results described in a previous report.[8]

Thermal Analyses. In general, an increase in the degree of intramolecular hydrogen bonding will decrease the surface free energy, whereas stronger intermolecular hydrogen bonding will enhance the thermal properties, such as the values of T_g and T_d and the char yield, of polymer blends and copolymer systems. We used DMA to examine the behavior of the glass transitions of the PVPh/PBZ copolymers (Figure 6). For the pure PBZ and pure PVPh, the values of T_g were 187 and 216 °C, respectively, as determined from the maxima of the tan δ plots. For the copolymers, the glass-transition behavior was similar to that of the surface free energy behavior: it first decreased upon increasing the PVPh content from 20 to 40 wt %. The PVPh/PBZ = 40/60 system exhibited the lowest value of T_g (166 °C), even lower than those of pure PVPh and pure PBZ. The value of T_g increased upon further increasing the PVPh content from 50 to 60 wt %—the highest value occurring for PVPh/PBZ = 60/40 (347 °C)—and then it decreased upon increasing the PVPh content from 70 to 100 wt %. Table 1 and Figure 6b summarize the values of T_g at various PVPh contents.

Figure 7 displays TGA thermograms of pure PBZ, pure PVPh, and their corresponding copolymers. For pure PBZ and pure PVPh, the values of T_d were 380 and 366 °C, respectively, as determined from their 20 wt % losses; their char yields were 36.8 and 20.2 wt %, respectively. Table 1 summarizes these data for the copolymers. Again, the behavior of the thermal decomposition temperatures and char yields followed a similar trend as that of the surface free energy: initial minima at a PVPh content of 20 wt % increases upon further increasing the PVPh contents from 30 to 60 wt %—with the highest values of T_d (410 °C) and char yield (47.8 wt %) for PVPh/PBZ = 60/40—and then decreases upon increasing the PVPh content from 70 to 100 wt %. Figure 8 displays the curing exotherms of the neat BA-m and the binary mixtures at various weight ratios of BA-m and PVPh. The curing exotherm of the

SCHEME 2: Possible Structures of PVPh/PBZ Copolymers at Various PVPh Contents

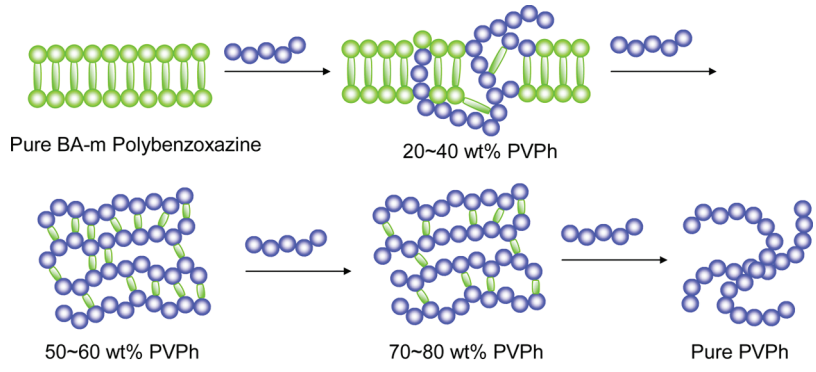

synthesized BA-m revealed an onset temperature of 170 °C with a peak temperature of 213 °C. The curing peak shifted to lower a temperature upon increasing the PVPh content in the binary mixture; that is, it shifted from 213 °C for BA-m to a low of 187 °C for PVPh/PBZ = 80/20. This accelerated curing suggests that PVPh acted as an initiator for the polymerization of the benzoxazine resin.[48] Although benzoxazine resin can be thermally cured, PVPh does not undergo curing in the absence of a cross-linker.[49] In terms of the breadth of the exotherms, the curing peaks for the binary mixtures broadened upon increasing the PVPh content.[50] Furthermore, the area under the exothermal peaks decreased from 347 J/g for the pure BA-m to 317 J/g for a PVPh content of 20 wt %. It then increased upon increasing the PVPh content from 30 to 60 wt %—with the highest curing area (475 J/g) occurring for PVPh/PBZ = 50/50—and then it decreased again upon increasing the PVPh content from 60 to 80 wt %, reaching a value of 337 J/g for PVPh/PBZ = 80/20 (Figure 9). This behavior suggests that only a certain fraction of the PVPh contributed to the exothermic network formation reaction in the binary blend.

In summary, the sample displaying the highest surface energy would exhibit the highest values of T_g, T_d, and char yield and the greatest cross-linking density because it would contain the highest fraction of intermolecular OH···O hydrogen bonds; Table 1 reveals that this sample was PVPh/PBZ = 60/40. In terms of mole percentage, PVPh/PBZ = 60/40 contains its PVPh and PBZ components at close to a 2:1 molar ratio, implying that two PVPh units reacted with one BA-m unit. As a result, Scheme 2 presents our proposed chain behavior of the PVPh/PBZ copolymers at various PVPh contents. We emphasize that PBZ reacts with PVPh through its phenolic OH groups, as indicated in Scheme 1.[50,51] Pure PBZ displays a regular network structure with a value of T_g of 187 °C; this structure would be destroyed upon increasing the content of PVPh polymer chains at lower PVPh contents (20−40 wt %), resulting in lower values of T_g and surface free energy because of the decreasing number of intermolecular hydrogen-bonding interactions. Further increases in the PVPh content, from 50 to 80 wt %, resulted in PVPh becoming the major matrix (continuous phase), with BA-m acting as a cross-linking agent (dispersion phase).[52] As a result, the PVPh/PBZ = 60/40 sample (2:1 molar ratio) exhibited the highest values of T_g, T_d, char yield, and surface free energy because of its complete curing and highest cross-linking density. Subsequently, the thermal properties decreased upon further increasing the PVPh content because the cross-linking density decreased at PVPh contents of 70−80 wt %.

Conclusions

Decreasing the fraction of intermolecular hydrogen bonds between the OH groups in PVPh/PBZ blends tends to decrease the surface free energy. The lowest surface free energy (16.8 mJ/m^2) occurred for the PVPh/PBZ = 30/70 system; this value is even lower than that of PTFE (22.0 mJ/m^2). In contrast, increasing the degree of intermolecular hydrogen bonding enhances the thermal properties of PVPh/PBZ blends. As a result, controlling the extent of intermolecular hydrogen bonding allows the surface free energy and thermal properties to be optimized. This approach is a new way to prepare new classes of low-surface-energy materials.

Acknowledgment. This study was supported financially by the National Science Council, Taiwan, Republic of China, under contracts NSC97-2221-E-110-013-MY3, NSC98-2221-E-110-006, and NSC 98-2120-M-009-001. The authors would like to thank Dr. Han-Ching Lin and Professor Feng-Chih Chang of the Department of Applied Chemistry, National Chiao-Tung University in Taiwan, for their helpful discussion.

References and Notes

(1) Coulson, S. R.; Woodward, I.; Badyal, J. P. S.; Brewer, S. A.; Willis, C. *J. Phys. Chem. B* **2000**, *104*, 8836.
(2) Jin, M.; Feng, X.; Xi, J.; Zhai, J.; Cho, K.; Feng, L.; Jiang, L. *Macromol. Rapid Commun.* **2005**, *26*, 1805.
(3) Feng, L.; Zhang, Z.; Mai, Z.; Ma, Y.; Liu, B.; Jiang, L.; Zhu, D. *Angew. Chem., Int. Ed.* **2004**, *43*, 2012.
(4) Hillborg, H.; Tomczak, N.; Olah, A.; Schonherr, H.; Vancso, G. J. *Langmuir* **2004**, *20*, 785.
(5) Wu, S. *Polymer Interface and Adhesion*; Marcel Dekker: New York, 1982.
(6) Feiring, A. E.; Imbalzano, J. F.; Kerbow, D. L. *Adv. Fluoroplast. Plast. Eng.* **1994**, 27.
(7) Carlson, D. P.; Schmiegel, W. *Ullmann's Encyclopedia of Industrial Chemistry*; VCH Verlagsgesellschaft: Weinheim, Germany, 1988; p 393.
(8) Wang, C. F.; Su, Y. C.; Kuo, S. W.; Huang, C. F.; Sheen, Y. C.; Chang, F. C. *Angew. Chem., Int. Ed.* **2006**, *45*, 2248.
(9) Kobayashi, H.; Owen, M. J. *Trends Polym. Sci.* **1995**, *3*, 5.
(10) Schmidt, D. L.; Coburn, C. E.; DeKoven, B. M.; Potter, G. E.; Meyers, G. F.; Fischer, D. A. *Nature* **1994**, *368*, 41.
(11) Owen, M. J. *Comments Inorg. Chem.* **1988**, *7*, 195.
(12) Ma, K. X.; Chung, T. S. *J. Phys. Chem. B* **2001**, *105*, 4145.
(13) Wang, C. F.; Su, Y. C.; Huang, C. F.; Chang, F. C. *Macromol. Rapid Commun.* **2006**, *27*, 336.
(14) Wang, C. F.; Wang, Y. T.; Tung, P. H.; Kuo, S. W.; Lin, C. H.; Sheen, Y. C.; Chang, F. C. *Langmuir* **2006**, *22*, 8289.
(15) Liao, C. S.; Wang, C. F.; Lin, H. C.; Chou, H. Y.; Chang, F. C. *Langmuir* **2009**, *25*, 3359.
(16) Liao, C. S.; Wang, C. F.; Li, H. C.; Chou, H. Y.; Chang, F. C. *J. Phys. Chem. C* **2009**, *112*, 16189.
(17) Wang, C. F.; Chiou, S. F.; Ko, F. H.; Chen, J. K.; Chou, C. T.; Huang, C. F.; Kuo, S. W.; Chang, F. C. *Langmuir* **2007**, *23*, 5868.
(18) Lin, H. C.; Wang, C. F.; Kuo, S. W.; Tung, P. H.; Huang, C. F.; Lin, C. H.; Chang, F. C. *J. Phys. Chem. B* **2007**, *111*, 3404.
(19) Low, H. Y.; Ishida, H. *Polym. Degrad. Stab.* **2006**, *91*, 805.
(20) Tsibouklis, J.; Graham, P.; Eaton, P. J.; Smith, J. R.; Nevell, T. G.; Smart, J. D.; Ewen, R. J. *Macromolecules* **2000**, *33*, 8460.
(21) Kuo, S. W. *J. Polym. Res.* **2008**, *15*, 459.
(22) Kuo, S. W.; Tung, P. H.; Chang, F. C. *Macromolecules* **2006**, *39*, 9388.
(23) Kuo, S. W.; Lee, H. F.; Huang, C. F.; Huang, C. J.; Chang, F. C. *J. Polym. Sci., Part A: Polym. Chem.* **2008**, *46*, 3108.
(24) Goward, G. R.; Sebastiani, D.; Schnell, I.; Spiess, H. W.; Kim, H. D.; Ishida, H. *J. Am. Chem. Soc.* **2003**, *125*, 5792.
(25) Goward, G. R.; Schnell, I.; Brown, S. P.; Spiess, H. W.; Kim, H. D.; Ishida, H. *Magn. Reson. Chem.* **2001**, *125*, 5792.
(26) Schnell, I.; Brown, S. P.; Low, H. Y.; Ishida, H.; Spiess, H. W. *J. Am. Chem. Soc.* **1998**, *120*, 11784.
(27) Kim, H. J.; Brunovska, Z.; Ishida, H. *Polymer* **1999**, *40*, 6565.
(28) Hemvichian, K.; Kim, H. D.; Ishida, H. *Polym. Degrad. Stab.* **2005**, *87*, 213.
(29) Hemvichian, K.; Laobuthee, A.; Chirachanchai, S.; Ishida, H. *Polym. Degrad. Stab.* **2002**, *76*, 1.
(30) Kuo, S. W.; Lee, H. F.; Huang, W. J.; Jeong, K. U.; Chang, F. C. *Macromolecules* **2009**, *42*, 1619.
(31) Kuo, S. W.; Cheng, R. S. *Polymer* **2009**, *50*, 177.
(32) Chen, W. C.; Kuo, S. W.; Jeng, U. S.; Chang, F. C. *Macromolecules* **2008**, *41*, 1401.
(33) Chen, S. C.; Kuo, S. W.; Liao, C. S.; Chang, F. C. *Macromolecules* **2008**, *41*, 8865.
(34) Kuo, S. W.; Lin, C. L.; Chang, F. C. *Polymer* **2002**, *43*, 3943.
(35) Kuo, S. W.; Chang, F. C. *Macromolecules* **2001**, *34*, 5224.
(36) Kuo, S. W.; Chang, F. C. *Polymer* **2003**, *44*, 3021.
(37) Lin, C. L.; Chen, W. C.; Liao, C. S.; Su, Y. C.; Huang, C. F.; Kuo, S. W.; Chang, F. C. *Macromolecules* **2005**, *38*, 6435.
(38) Fowkes, F. W. In *Adhesion and Adsorption of Polymers, Polymer Science and Technology*; Lee, L. H., Ed.; Plenum Press: New York, 1980; Vol. 12A, p 43.
(39) Drelich, J.; Miller, J. D.; Good, R. J. *J. Colloid Interface Sci.* **1996**, *179*, 37.
(40) Good, R. J.; van Oss, C. J. In *Modern Approaches to Wettability: Theory and Applications*; Schrader, M. E., Loeb, G., Eds.; Plenum Press: New York, 1992; pp 1−27.
(41) Yoshimasa, U.; Takashi, N. *Langmuir* **2005**, *21*, 2614.
(42) Dunkers, J.; Ishida, H. *Spectrochim. Acta* **1995**, *51A*, 855.
(43) Choperena, A.; Painter, P. *Macromolecules* **2009**, *42*, 6159.
(44) Kim, H. D.; Ishida, H. *J. Phys. Chem. A* **2002**, *106*, 3271.

(45) Noda, I.; Ozaki, Y. *Two-Dimensional Correlation Spectroscopy*; John Wiley & Sons Ltd.: Chichester, U.K., 2004.
(46) Kuo, S. W. *Polymer* **2008**, *49*, 4420.
(47) Noda, I. *J. Am. Chem. Soc.* **1989**, *111*, 8116.
(48) Kuo, S. W.; Huang, C. F.; Tung, P. H.; Huang, W. J.; Huang, J. M.; Chang, F. C. *Polymer* **2005**, *46*, 9348.
(49) Rimdusit, S.; Ishida, H. *Polymer* **2000**, *41*, 7941.
(50) Takeichi, T.; Kawauchi, T.; Agag, T. *Polym. J.* **2008**, *40*, 1121.
(51) Agag, T.; Takeichi, T. *High Perform. Polym.* **2001**, *13*, S327.
(52) Ergin, M.; Kiskan, B.; Gacal, B.; Yagci, Y. *Macromolecules* **2007**, *40*, 4724.

JP9059642